Available online at www.sciencedirect.com
SCIENCE DIRECT
Intermetallics 13 (2005) 1141–1145
Intermetallics
www.elsevier.com/locate/intermet

Structure and electrochemical characteristics of $Ti_{0.25-x}Zr_xV_{0.35}Cr_{0.1}Ni_{0.3}$($x=0.05$–$0.15$) alloys

Yujun Chai[a], Wenya Yin[a], Zhiying Li[b], Xinbo Zhang[a], Minshou Zhao[a,*]

[a]*Key Laboratory of Rare Earth Chemistry and Physics, Changchun Institute of Applied Chemistry, Chinese Academic of Sciences, Changchun 130022, China*
[b]*State Key Laboratory of Electroanalytical Chemistry, Changchun Institute of Applied Chemistry, Chinese Academic of Sciences, Changchun 130022, China*

Received 1 March 2004; accepted 8 February 2005
Available online 23 May 2005

Abstract

The structure and electrochemical properties of the $Ti_{0.25-x}Zr_xV_{0.35}Cr_{0.1}Ni_{0.3}$($x=0.05$–$0.15$) alloy electrodes have been investigated. These alloys mainly consist of a V-based solid solution with BCC structure and a C14 Laves phase with hexagonal structure as determined by X-ray diffraction analysis. Scanning electron micrographs show that these alloys form dendritic crystal. The discharge capacities of the alloys increase with increasing temperature from 303 to 333 K, and then decrease while the temperature is above 333 K. The cycle life, the rate capability and the electrochemical impedance spectra are also investigated. The Laves phase as electrocatalyst increases the fresh surface during charging-discharging process, improving the electrochemical performance of these alloy electrodes.

Keywords: A. Multiphase intermetallics; B. Hydrogen storage

1. Introduction

Vanadium and vanadium-based solid solution alloys have attracted considerable research interest due to higher hydrogen storage capacity. Takahashi and coworkers [1,2] reported that the electrodes of $V_3TiNi_{0.56}$ and $V_3TiNi_{0.56}Hf_{0.24}$ alloys had higher discharge capacity than other hydrogen storage alloys, and Lei et al. further studied the effect of Mn and Cr on the performance of $V_3TiNi_{0.56}Hf_{0.24}$ hydride electrode [3,4]. Iwakura et al. [5] studied the properties of $TiV_{2.1}Ni_{0.3}$ hydrogen storage alloy and found that the discharge capacity of the alloy electrode reached 540 mAh/g at a small discharge current density. Furthermore, Lei et al. [6] discussed the effect of Ni on the properties of $TiV_{2.1}$ and pointed out that $TiV_{2.1}Ni_{0.5}$ had high discharge capacity and high-rate discharge capability. For other V-based alloys, few investigations have been presented. Recently, the Ti–V-based alloys, such as Ti–V–Cr, Ti–V–Mn reported by Akiba, are demonstrated to absorb/desorb an appreciable amount of hydrogen, and the most effective hydrogen storage capacity is about 2.2 mass% [7,8]. However, few papers are concerned with the electrochemical characteristics of Ti–V–Cr alloy. The electrochemical performance of the Ti–V–Cr–Ni alloy as metal hydride electrode had been studied and the maximum discharge capacity of 240 mAh/g has been obtained at 313 K for $Ti_{0.25}V_{0.35}Cr_{0.1}Ni_{0.3}$ in our research group.

In order to improve the property of the alloy electrode further, zirconium is used to substitute for titanium. In this paper, the structures and electrochemical characteristics of $Ti_{0.25-x}Zr_xV_{0.35}Cr_{0.1}Ni_{0.3}$($x=0.05$–$0.15$) alloys are discussed.

2. Experimental

The samples of $Ti_{0.25-x}Zr_xV_{0.35}Cr_{0.1}Ni_{0.3}$($x=0.05$–$0.15$) alloys were melted by arc melting under an argon atmosphere. In order to acquire a homogeneous alloy, the alloy ingots were turned over and remelted at least four times. Then the as-cast alloys were crushed mechanically in air and further pulverized with a ceramic mortar to 300 meshes. The electrodes were prepared by mixing the alloy powder with porous nickel powder in a weight ratio of 1:5 and cold-pressing the mixture to form pellets. Prior to

* Corresponding author. Tel.: +86 431 5262365; fax: +86 431 5698041.
E-mail address: zhaoms@ciac.jl.cn (M. Zhao).

0966-9795/$ - see front matter © 2005 Elsevier Ltd. All rights reserved.
doi:10.1016/j.intermet.2005.02.005

electrochemical testing, all alloy electrodes were activated by immersion in 6 M KOH aqueous solution for two days. The positive electrode was a sintered Ni $(OH)_2$/NiOOH plate. The charge/discharge tests were carried out with DC-5 battery testing instrument under computer control. The alloy electrodes were charged with a current density of 120 mA/g and discharged with a current density of 60 mA/g to a cut-off voltage of 0.8 V in a water-bath.

The X-ray diffraction (XRD) analysis was used to evaluate the crystal structure of the $Ti_{0.25-x}Zr_xV_{0.35}Cr_{0.1}Ni_{0.3}$ alloys. The experiment was carried out on a RIGAKU D/max-IIB X-ray diffractometer with Cu Kα radiation at 40 kV and 200 mA. Scanning electron microscopy (SEM) was used to study the microstructure of the solid solution alloy. Electrochemical impedance spectroscopy (EIS) measurements were conducted using a Solartron 1470 battery test unit with a 1255B frequency response analyzer. The EIS spectra were obtained in the frequency range of 10^5–10^{-2} Hz with ac amplitude perturbation of 5 mV for a depth of discharge of 50% under open circuit condition.

3. Result and discussion

3.1. Structure

It is well known that zirconium has a strong tendency to form Laves phase [9]. When titanium is partially substituted by zirconium, the peaks of the C14 Laves phase appear. The XRD patterns of $Ti_{0.25-x}Zr_xV_{0.35}Cr_{0.1}Ni_{0.3}$($x$=0.05–0.15) alloys are shown in Fig. 1. It can be seen that the alloys are mainly composed of a V-based solid solution phase with body-centered cubic (BCC) structure and C14 Laves phase with a hexagonal structure. When x=0.05, the peaks of Laves phase are not discernible. With increasing x,

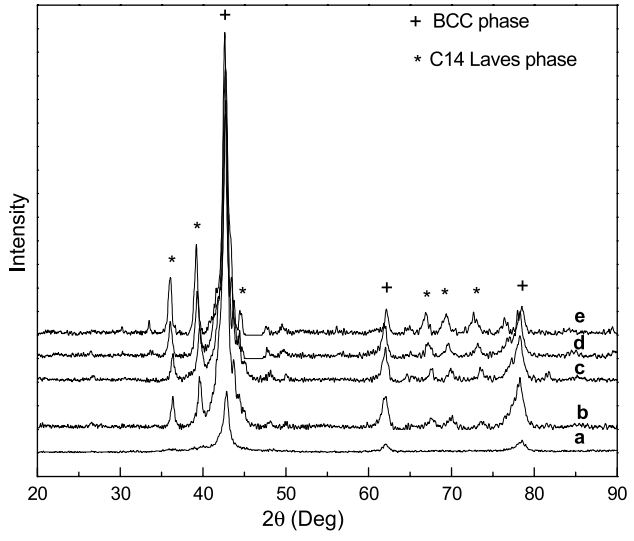

Fig. 1. XRD patterns of $Ti_{0.25-x}Zr_xV_{0.35}Cr_{0.1}Ni_{0.3}$($x$=0.05–0.15) alloys (a, 0.05; b, 0.07; c, 0.08; d, 0.10; e, 0.15).

Table 1
Compositions and lattice parameters of $Ti_{0.25-x}Zr_xV_{0.35}Cr_{0.1}Ni_{0.3}$($x$=0.05–0.15) alloys

X	Phase	Lattice parameter		Unit cell ($\times10^{-3}$ nm^3)	Molar fraction
		a	c		
0.05	BCC	0.2985		26.60	
	BCC	0.2991		26.76	0.74
0.07	C14 phase	0.2940	0.8038	60.18	0.26
	BCC	0.2994		26.84	0.71
0.08	C14 phase	0.2945	0.8038	60.39	0.29
	BCC	0.2995		26.87	0.67
0.10	C14 phase	0.2977	0.8064	61.91	0.33
	BCC	0.2981		26.49	0.51
0.15	C14 phase	0.2980	0.8105	62.35	0.49

the peaks of the Laves phase appear and shift to the low angle. The volume fraction and the lattice parameter of the Laves phase increase as shown in Table 1. Moreover, the lattice parameter of V-based solid solution increases slightly when x increases from 0.05 to 0.10 and decreases as x increases further. It is probable that some zirconium solutes enter the solid solution and cause the lattice swelling due to the partial substitution of zirconium for titanium, while the majority of zirconium forms the C14 Laves phase with other elements. When the content of zirconium is greater than 0.15, more elements dissolve in the Laves phase, and thus make the element in solid solution alloy change.

The SEM micrographs of $Ti_{0.25-x}Zr_xV_{0.35}Cr_{0.1}Ni_{0.3}$($x$=0.05–0.15) alloys are shown in Fig. 2. The content of zirconium has a pronounced effect on the structure of the alloy. It can be seen from the photographs that the alloys have a dendritic structure when x=0.05–0.07, but form columnar crystals when x=0.08–0.15, and the grain size decreases when x increases.

3.2. Electrochemical property

Fig. 3 shows the dependence of discharge capacity on cycle number for $Ti_{0.25-x}Zr_xV_{0.35}Cr_{0.1}Ni_{0.3}$($x$=0.05–0.15) alloy electrodes at 313 K. It can be seen that the activation property worsens slightly as x increases. The discharge capacity increases with changing x from 0.05 to 0.15 after the electrode is activated, and the cyclic stability of these alloy electrodes is good. In the KOH electrolyte solution, the single solid solution phase has little electrochemical discharge capability because it does not have electrocatalytic activity. However, the C14 Laves phase can act as the electrocatalyst and micro-current collector and make the alloy reversibly absorb/desorb hydrogen [3]. The C14 Laves phase is present in the $Ti_{0.25-x}Zr_xV_{0.35}Cr_{0.1}Ni_{0.3}$($x$=0.05–0.15) alloys as mentioned above, and the content of the C14 Laves phase increases as x increases. The contents of solid solution and C14 Laves phase in the alloys are evaluated semi-quantitatively from the peak intensity in XRD patterns. When the molar ratio of the solid solution and Laves phase is less than 3 and greater than 1, the discharge

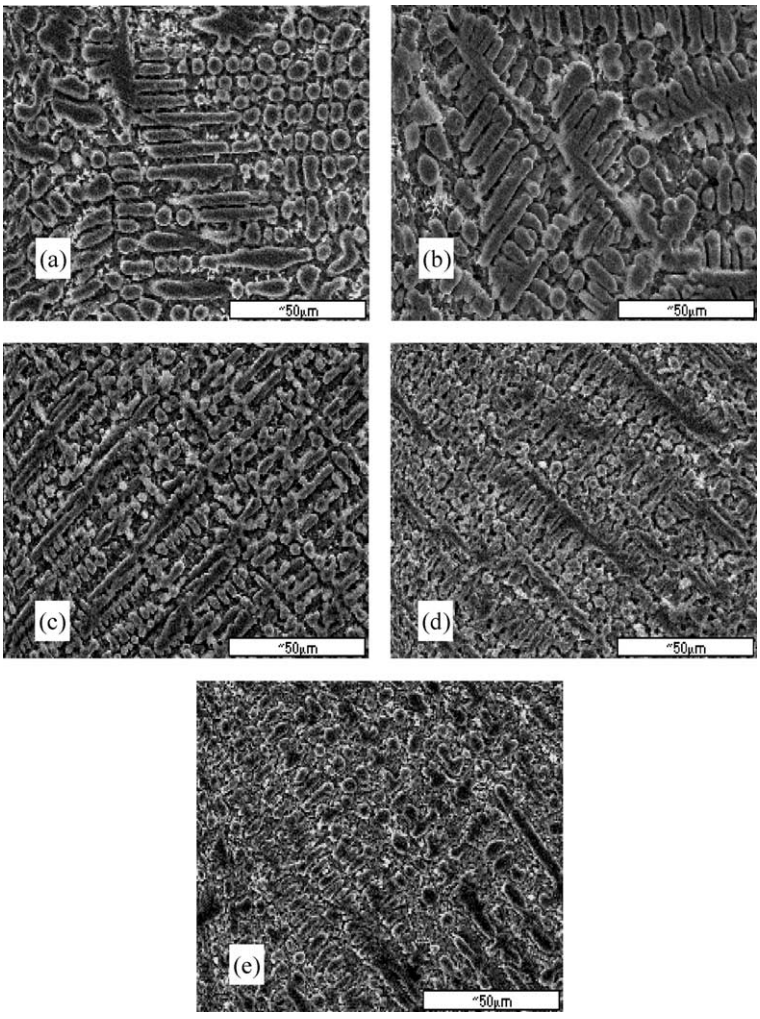

Fig. 2. SEM micrographs of $Ti_{0.25-x}Zr_xV_{0.35}Cr_{0.1}Ni_{0.3}$($x$=0.05–0.15) alloys (a, 0.05; b, 0.07; c, 0.08; d, 0.10; e, 0.15).

capacity only changes a little, which implies a correlation between the discharge capacity and the fraction of the phases in the alloys. In the meantime the presence of chromium limits the corrosion of vanadium and also leads to improved cyclic stability [10].

All measurements of discharge capacity were conducted by charging at ambient temperature and discharging at various temperatures. The dependence of the discharge capacity of these alloys on temperature is shown in Fig. 4. It can be seen that the discharge capacity changes slightly at 303–323 K, and it evidently increases at 333 K and the maximum discharge capacity of 350 mAh/g is observed. However, the discharge capacity decreases when the temperature is above 333 K.

Fig. 5 gives the relation between the discharge capacity and the discharge current density. The discharge capacity increases with increasing x, which is perhaps related to the content of the Laves phase. The Laves phase accelerates the cracking of the alloys, and creates more fresh surface, which is the specific reaction surface that affects the rate capability [11,12].

The electrochemical impedance spectra of $Ti_{0.25-x}Zr_xV_{0.35}Cr_{0.1}Ni_{0.3}$($x$=0.05–0.15) alloy electrodes at a DOD (depth of discharge) of 50% is shown in Fig. 6. It is demonstrated that the spectra of all metal hydride consist of

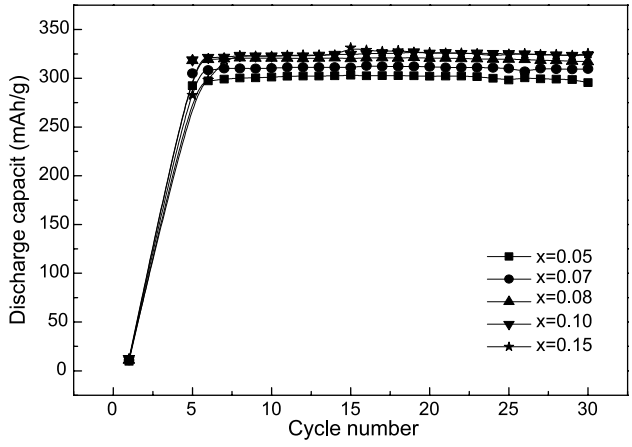

Fig. 3. Dependence of discharge capacity on cycle number for $Ti_{0.25-x}Zr_xV_{0.35}Cr_{0.1}Ni_{0.3}$($x$=0.05–0.15) alloy electrodes at 313 K.

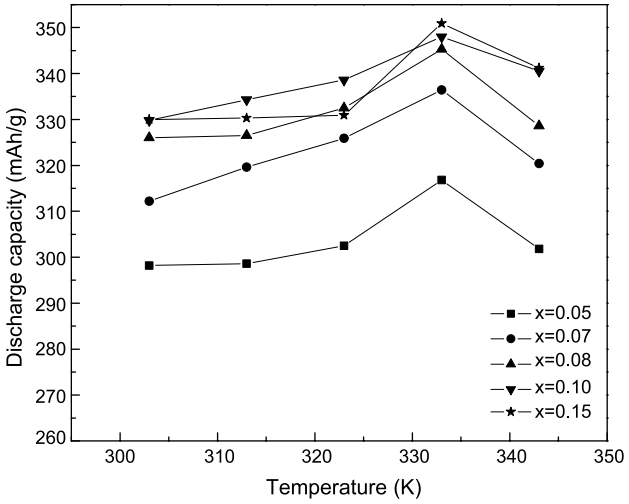

Fig. 4. Dependence of discharge capacity with a discharge current density of 60 mA/g on temperature for $Ti_{0.25-x}Zr_xV_{0.35}Cr_{0.1}Ni_{0.3}$($x$=0.05–0.15) alloy electrodes.

two semicircles at high frequency and a straight line at low frequency. The first semicircle looks like a straight line, which may be related to the porosity effect of the alloy electrode. The radius of the second semicircle decreases as x changes from 0.05 to 0.08, then changes slightly. The equivalent circuit proposed by Kuriyama and coworkers for the alloy electrode is shown in Fig. 7 [13]. $R1$ is the electrolyte resistance. $R2$ and $Q2$ characterize the contact resistance and the contact capacitance between the current collector and the alloy pellet, respectively, which corresponds to the semicircle in the high frequency region. The contact resistance and the contact capacitance between alloy powders in the electrode pellet are described by $R3$ and $C3$, respectively. $R4$ and $Q4$ present the charge-transfer resistance and the double-layer capacitance, respectively,

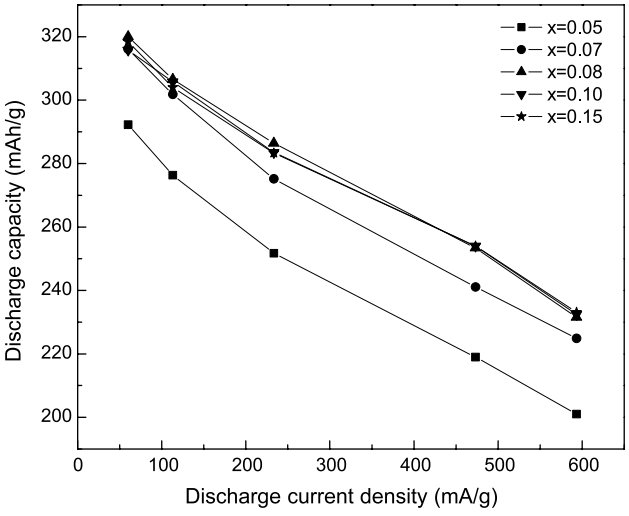

Fig. 5. Relation between the discharge capacity and the discharge current density for $Ti_{0.25-x}Zr_xV_{0.35}Cr_{0.1}Ni_{0.3}$($x$=0.05–0.15) alloy electrodes.

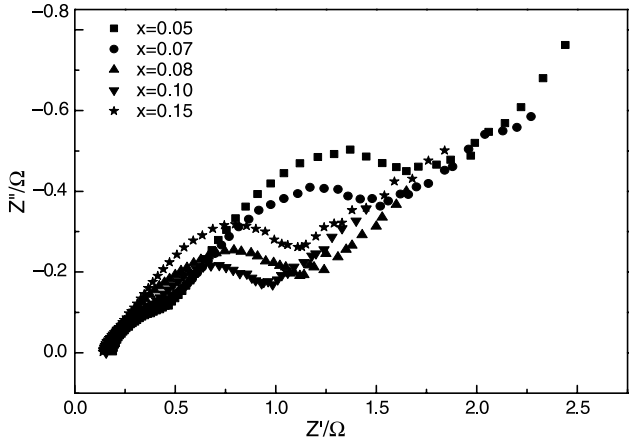

Fig. 6. Electrochemical impedance spectra of $Ti_{0.25-x}Zr_xV_{0.35}Cr_{0.1}Ni_{0.3}$ (x=0.05–0.15) alloy electrodes.

which is characterized by the second semicircle. W is the Warburg resistance, which is due to the hydrogen diffusion process in the alloy electrode. The fit results by least square method according to this model are shown in Fig. 8. It is evident that the electrolyte resistance $R1$ and the contact resistances $R2$ and $R3$ are almost independent of x. However, the charge-transfer resistance $R4$ decreases markedly as x changes from 0.05 to 0.08 and then decreases slightly, which corresponds to the result mentioned above. These results indicate that the electrochemical

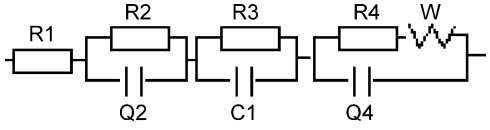

Fig. 7. Equivalent circuit of $Ti_{0.25-x}Zr_xV_{0.35}Cr_{0.1}Ni_{0.3}$($x$=0.05–0.15) alloy electrodes.

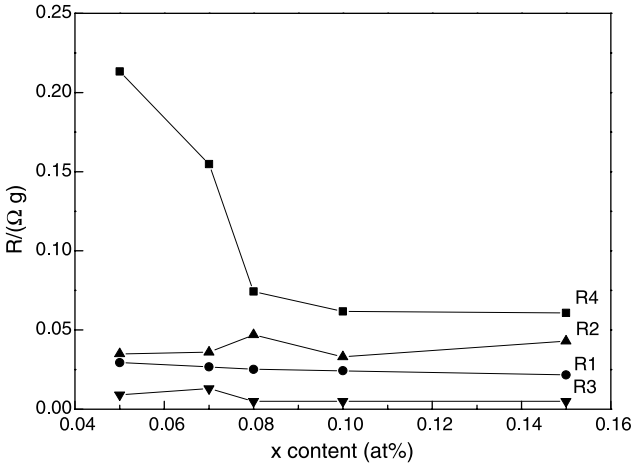

Fig. 8. Resistive component for $Ti_{0.25-x}Zr_xV_{0.35}Cr_{0.1}Ni_{0.3}$($x$=0.05–0.15) metal hydride. ($R1$, the electrolyte resistance; $R2$ $R3$, the contact resistances; $R4$, the charge-transfer resistance).

activity is close to the charge-transfer resistance on the alloy surface.

From the above result, it can be understood that the substitution of zirconium for titanium changes the charge-transfer resistance, decreases the electrochemical reaction resistance, and enhances the discharge capacity and rate capability.

4. Conclusion

The structures and the electrochemical properties of the $Ti_{0.25-x}Zr_xV_{0.35}Cr_{0.1}Ni_{0.3}$($x$=0.05–0.15) electrode alloys have been investigated in this work. These alloys mainly consist of a V-based solid solution with BCC structure and a C14 Laves phase with hexagonal structure, and form dendritic crystal. The discharge capacity and the rate capability of the alloy increase when x changes from 0.05 to 0.15, but the change is small when x varies from 0.8 to 0.15. The discharge capacity is dependent on temperature and is enhanced with increasing temperature from 303 to 333 K; the maximum discharge capacity of 350 mAh/g is obtained at 333 K, and then decreases. The EIS results show that the charge-transfer resistance decreases markedly with increasing x from 0.05 to 0.08 and then decreases slowly.

Acknowledgements

This work is supported by the National Natural Science Foundation of China (grant No. 20171042).

References

[1] Tsukahara M, Takahashi K, Mishima T, Isomura A, Sakai T. J Alloys Compd 1996;243:133.
[2] Tsukahara M, Takahashi K, Mishima T, Sakai T, Miyamura H, Kuriyama N, Uehara I. J Alloys Compd 1995;224:162.
[3] Zhang QA, Lei YQ, Yang XG, Du YL, Wang QD. Int J Hydrogen Energy 2000;25:977.
[4] Zhang QA, Lei YQ, Yang XG, Du YL, Wang QD. Int J Hydrogen Energy 2000;25:657.
[5] Iwakura C, Kyung W, Miyauchi R, Inoue H. J Electrochem Soc 2000; 147:2503.
[6] Guo R, Chen LX, Lei YQ, Liao B, Ying T, Wang QD. Int J Hydrogen Energy 2003;28:803.
[7] Akiba E, Iba H. Intermetallics 1998;6:461.
[8] Cho SW, Han CS, Park CN, Akiba E. J Alloys Compd 1999;288:294.
[9] Ovshinsky SR, Fetcenko MA, Poss J. Nature 1993;260:176.
[10] Park HY, Chang I, Cho WE, Cho BW, Jang H, Lee SR, et al. J Int Hydrogen Energy 2001;26:949.
[11] Tsukahara M, Tsukahara K, Takahash K, Mishima T, Isomura A, Sakai T. J Alloys Compd 1996;236:151.
[12] Kim DM, Jang KJ, Lee JY. J Alloys Compd 1999;293–295:583.
[13] Kuriyanma N, Sakai T, Miyamura H, Uehara I, Ishikawa H, Iwasaki T. J Alloys Compd 1993;202:183.